

## Article

# New insight into iron biogeochemical cycling in soil-rice plant system using iron isotope fractionation

Guojun Chen<sup>a,1</sup>, Tongxu Liu<sup>a,1</sup>, Yongzhu Li<sup>a</sup>, Ting Gao<sup>b</sup>, Fang Huang<sup>c</sup>, Xiaomin Li<sup>d</sup>, Songxiong Zhong<sup>a</sup>, Fangbai Li<sup>a,\*</sup>

<sup>a</sup> National-Regional Joint Engineering Research Center for Soil Pollution Control and Remediation in South China, Guangdong Key Laboratory of Integrated Agro-environmental Pollution Control and Management, Institute of Eco-environmental and Soil Sciences, Guangdong Academy of Sciences, Guangzhou 510650, China

<sup>b</sup> State Key Laboratory of Environmental Geochemistry, Institute of Geochemistry, Chinese Academy of Sciences, Guiyang 550081, China

<sup>c</sup> CAS Key Laboratory of Crust–Mantle Materials and Environments, School of Earth and Space Sciences, University of Science and Technology of China, Hefei 230026, China

<sup>d</sup> SCNU Environmental Research Institute, Guangdong Provincial Key Laboratory of Chemical Pollution and Environmental Safety & MOE Key Laboratory of Theoretical Chemistry of Environment, South China Normal University, Guangzhou 510006, China



## ARTICLE INFO

## Keywords:

Fe uptake and transport  
Rice plants  
Fe isotope fractionation  
Stele and cortex  
Phloem and xylem

## ABSTRACT

Iron (Fe) migration in soil-plants is a critical part of Fe biogeochemical cycling in the earth surface system. Fe isotope fractionation analysis in the soil-rice system is promising for quantitatively assessing various pathways and clarifying Fe transformation processes. However, the mechanisms of Fe isotope fractionation in the soil-rice system are not well understood. In this study, the Fe isotopic compositions ( $\delta^{56}\text{Fe}$ ) of rhizosphere soils, pore water, Fe plaque, and rice plant tissues at the jointing and mature stages of the plants were determined. The rice plants were slightly enriched in heavier  $\delta^{56}\text{Fe}$  by  $\sim 0.3\%$  relative to the soil, and the stele and cortex showed similar  $\delta^{56}\text{Fe}$  values, indicating that the uptake of Fe by rice plants predominantly occurred via Fe(III)-phytosiderophores (Fe(III)-PS) chelation, but not Fe(III) reduction. Additionally, at both the jointing and mature stages, the rice plant tissues showed similar  $\delta^{56}\text{Fe}$  values. However, the Fe isotope fractionation between the roots and stems ( $\Delta^{56}\text{Fe}_{\text{root-stem}}$ ) was  $1.39 \pm 0.13\%$ , which is similar to the previously *Ab initio*-calculated values between Fe(III)-citrate and Fe(III)-2-deoxymugineic acid (DMA), indicating that both the phloem and xylem have similar  $\delta^{56}\text{Fe}$  values, and the major Fe-chelating substances in the phloem of the rice plants are Fe(III)-DMA and Fe(II)-Nicotianamine (NA). Therefore, this study demonstrates that Fe isotope fractionation can be used as a signature for interpreting the Fe uptake and translocation mechanism in the soil-rice system.

## 1. Introduction

Iron is a vital plant micronutrient and an essential element in many physiological, metabolic, and biogeochemical processes [1]. For most plants, two specific mechanisms (Strategy I and Strategy II) for efficient Fe uptake have been reported [2]. For Strategy I-related plants (e.g., non-graminaceous plants and dicots), the pH decreased due to proton release by proton-ATPase and the Fe(III) was then reduced to Fe(II) through the inducible ferric chelate reductase activity of FRO2 [3]. Fe(II) is translocated into the cells of the plant roots by Fe(II) transporters [1]. On the other hand, for Strategy II-related plants (e.g., graminaceous monocots), mugineic acid-family phytosiderophores (PS) can be released and chelated with Fe(III) in rhizosphere soils [4], after which the Fe(III)-PS complex is then transported into the root cells. As an important cereal crop, rice plants serve as a stable food source for more

than half of the world population, and iron is an essential micronutrient needed for their growth and development [5]. Iron deficiency is one of the most widespread and serious problems associated with crop production and human nutrition in the world [6]. Additionally, high soil Fe concentrations and excessive Fe uptake cause Fe toxicity as well as the bronzing for rice plants, leading to a nutritional disorder in the rice plants [7]. This sophisticated Fe uptake and translocation plays an important role in maintaining Fe concentrations at physiologically optimal levels in rice plants [8]. Understanding the mechanism of Fe uptake and translocation of rice plants is critical to overcoming the problems related to rice plant Fe deficiency or toxicity. Additionally, understanding this mechanism has significant implications with respect to increasing rice yield and ensuring human health. In the soil-rice plant system, Fe(II) is usually the dominant form in flooded paddy soils. However, roots secrete oxygen and Fe(II) is oxidized into Fe(III) in the rhizosphere [9]. For rice, which is an example of a graminaceous plant, Fe uptake can occur via Strategy II [10]; however, Fe uptake for rice plants via Strategy I has also been observed [11]; it was reported that the mechanism of Fe uptake depends on the Fe availability in soils [12,13]. The mechanism of Fe

\* Corresponding author.

E-mail address: [cefbli@soil.gd.cn](mailto:cefbli@soil.gd.cn) (F. Li).

<sup>1</sup> These authors contributed equally to this work.

uptake and translocation in the soil-rice plant system is still not well understood.

Iron isotopes have been extensively used as signatures to clarify geochemical processes [14], and recently, they have been employed in the study of the mechanism of Fe uptake and translocation in plants [12,15–18]. For Strategy I-related plants, it has been reported that owing to the reduction of Fe(III), the magnitude of Fe isotope fractionation can reach up to 1.5‰ during Fe uptake and translocation, and there is a decrease in the Fe isotopic compositions ( $\delta^{56}\text{Fe}$ ) of the roots, stems, leaves, and seeds during Fe translocation [12]. For Strategy II-related plants, the magnitude of Fe isotope fractionation associated with Fe(III)-PS uptake and translocation is only 0.2–0.3‰, and during Fe translocation, the roots, stems, leaves, and seeds basically show similar  $\delta^{56}\text{Fe}$  values [12]. Hence, it is possible that Fe isotope fractionation is a potential indicator that can be used to clarify Fe availability in the plant substrate and the Fe uptake mechanism in plants.

Recently, it was proposed that higher degrees of Fe isotope fractionation (up to 1.54‰ within the plants) during Fe uptake and translocation in rice plants can be attributed to Strategy I, while lower degrees (~0.30‰ within the plants) can be attributed to Strategy II [11]. However, based on quantum chemical calculations, Fe isotope fractionation resulting from changes in Fe speciation without redox transformation can also be up to 1.5‰ [15], indicating that distinguishing Strategy I- and Strategy II-related plants based on the magnitude of Fe isotope fractionation is not always accurate. Fe in the rhizosphere must pass through the cell wall of the root cortex, and reach the plasma membrane of the root cells before entering the root stele [19]. For Strategy I-related plants, Fe(III) redox enzymes are present in the plasma membrane; thus, Fe(III) reduction occurs during Fe uptake from the cortex to the stele. Contrarily, for Strategy II-related plants, Fe(III) reduction does not occur during this process. Therefore, the Fe isotope fractionation between the cortex and the stele ( $\Delta^{56}\text{Fe}_{\text{cortex-stele}}$ ) can be used to directly determine the redox state of Fe and also distinguish Strategy I- and Strategy II-related plants.

After Fe uptake via the root system of the rice plants, the Fe is translocated from the roots to the stem via both the xylem and phloem [20]. In the xylem sap, where the pH is below 7, Fe is translocated as Fe(III)-citrate [21]; however, the fate of the Fe(III)-ligand complexes in the phloem sap is still unclear [5]. Both 2-deoxymugineic acid (DMA) and Nicotianamine (NA) play an essential role in Fe translocation in the phloem [22]. It was suggested that Fe may be primarily translocated as Fe(III)-DMA in the phloem [23,24], as Fe(II)-NA [8,25], or even as both of Fe(III)-DMA and Fe(II)-NA [26]. Given that different types of Fe(III)-ligands can induce different magnitudes of Fe isotope fractionation [15], the Fe isotope signature is a promising indicator that can be used in the determination of the types of Fe(III)-ligand complexes in the phloem sap.

In this study, Fe isotope fractionation in the paddy soil, pore water, Fe plaque, and the different rice plant tissues at the jointing and maturity stages of the rice plants in the soil-rice system were investigated. Thus, the objectives of this study were to: (1) determine the Fe isotope variations in the soil-rice plant system; (2) clarify the molecular Fe-uptake process from the cortex to the stele of the plant roots using Fe isotope fractionation; and (3) reveal the mechanism of Fe translocation in the different above-ground tissues of the rice plants.

## 2. Materials and methods

### 2.1. Rice plant sampling and preparation

Rice plants (*Oriza sativa* L.) were cultivated in a paddy field at the South China Agricultural University, Guangzhou, China (113°21'57"E-23°9'56"N). Six groups of rice plants were harvested and collected at the jointing stage (October 27, 2017) and the maturity stage (December 15, 2017) of the plants. These groups of rice plants during the jointing and the maturity stage were sampled at the same spot. The whole rice

plants were sampled in triplicates using a wooden shovel, after which they were stored at  $-4\text{ }^{\circ}\text{C}$ . The different tissues, including roots, stems, leaves, and panicles, were separated using a pair of ceramic scissors at the jointing stage, and in addition to these other tissues, the husks and seeds were also sampled at the maturity stage of the plants. The locations of stems and leaves samples at the jointing and the maturity stage are shown in Fig. S1. To remove soil particles, the roots were cleaned via ultrasonication, and the Fe plaques from the roots were extracted using 30 mL of 1 N HCl for 1 h following Garnier et al., (2017) [13]. The HCl concentration increased from 0.5 N to 1 N, and the extraction time increased from 30 min to 1 h to ensure complete dissolution of Fe plaque in this study. The Fe extraction method of DCB (the mixture of dithionite, citrate, and bicarbonate) was not used in this study because the chemical purity of the reactants was not high enough for the subsequent Fe isotopic composition measurements. Thereafter, the extracts were filtered through 0.22- $\mu\text{m}$  nylon filters, and the roots were rinsed three times with ultrapure water. The roots were then peeled off and separated into the cortex and stele using a plastic tweezers. All the samples were rinsed with ultrapure water and dried at  $80\text{ }^{\circ}\text{C}$  for 48 h before grinding in an agate mortar.

### 2.2. Soil sampling and preparation

The rhizosphere soil samples were collected using a wooden spoon and stored in polyvinyl chloride (PVC) tubes. The PVC tube was full of soil samples and it was sealed with polymeric membrane to ensure the soil below the surface was not contacted with air. Then, the soil was quickly frozen and stored at  $-80\text{ }^{\circ}\text{C}$  in the lab. Thereafter, 20 mL of 0.5 N HCl was added into 50 mL centrifuge tubes containing 1 g of the soil samples following Guelke et al. (2010) [27]. Before the experiments of HCl-extraction, the soil was unfrozen and the surface of soil samples was removed to avoid post-sampling Fe oxidation. After centrifugation (10000 g) for 10 min, the supernatants were collected and filtered using 0.22  $\mu\text{m}$  nylon filters, and the soil precipitates were washed with high-purity water (18.2 M $\Omega$ .cm, Milli-Q, Millipore, USA). The above centrifugation procedure was repeated twice. The residues were washed three times with high-purity water, and dried at  $80\text{ }^{\circ}\text{C}$  for 48 h before grinding in an agate mortar and sieving using a 100-mesh nylon sieve. All the pore water samples were collected using a ceramic tube sampler with a bore diameter of 2  $\mu\text{m}$  (Rhizosphere, Netherlands). One end of the ceramic tube of the sampler was inserted into the soil to a depth of 10 cm and the distance between the end of the ceramic tube and the center of rice plants was 5 cm. Thus, the samples of pore water were collected between 0 and 10 cm. The other end with a syringe needle was connected to a container in which vacuum has been made. The collected pore water samples were then filtered through 0.22  $\mu\text{m}$  nylon filters into pre-cleaned polytetrafluoroethylene (PFA) containers, and acidified to a pH of 2 using 1 N HNO<sub>3</sub>. There was very little pore water at the maturity stage. Thus, the pore water was only sampled at the jointing stage.

### 2.3. Fe isotope analysis

The pore water (20 mL), Fe plaque extract (5 mL), and HCl-extracted soil extract (10 mL) were evaporated in PFA beakers at  $80\text{ }^{\circ}\text{C}$ . Thereafter, they were dissolved in 2 mL 6 N HNO<sub>3</sub> on a hotplate at  $120\text{ }^{\circ}\text{C}$  for 24 h. The soil (5 mg) and rice plant tissue samples (200–500 mg) were treated with concentrated HF-HNO<sub>3</sub> (1:4), and digested using a Microwave digestion system (Milestone, Italy) at  $180\text{ }^{\circ}\text{C}$  for 30 min. The obtained solutions were transferred into PFA beakers and evaporated to dryness on a hotplate at  $80\text{ }^{\circ}\text{C}$ . Thereafter, they were dissolved in a 3:1 (v/v) mixture of HCl-HNO<sub>3</sub>, and heated at  $140\text{ }^{\circ}\text{C}$  for 1–2 days until dryness. The HCl, HNO<sub>3</sub>, and HF were all distilled by sub-boiling distillation (DST-1000, Savilleux, USA) before sample digestion and Fe purification. Subsequently, 2 mL of 30% H<sub>2</sub>O<sub>2</sub> was added into the dried residue to remove the remaining organic matter. All the samples obtained after the

digestion were then re-dissolved in 6 N HCl for Fe separation and purification using an anion exchange resin (Bio-Rad AG1 × 8, 200 mesh) in a polypropylene column. The samples containing 50 μg of Fe were loaded, and the resin was rinsed with 4 mL of 6 N HCl. During this step, interfering elements and matrix components were eluted, and the retained Fe was then eluted with 4 mL of 0.4 N HCl, 1 mL of 8 N HNO<sub>3</sub>, and 0.5 mL of high-purity water. The Fe recovery rate from the column after purification was above 98%.

The Fe concentration was determined by Inductively Coupled Plasma-Optical Emission Spectroscopy (ICP-OES, Perkin Elmer Sciex, USA). The Fe concentration of standard materials of citrus leaf (GSB-11) has been measured. The Fe concentration of GSB-11 was 470 ± 11 mg kg<sup>-1</sup>, which was identical within error to the recommended value (480 ± 30 mg kg<sup>-1</sup>). Fe isotopic compositions were measured using a Neptune Plus Multi-Collector Inductively Coupled Plasma-Mass Spectrometer (MC-ICP-MS, Thermo Fisher Scientific, Bremen, Germany) at the Chinese Academy of Sciences Key Laboratory of Crust-Mantle Materials and Environments at the University of Science and Technology of China (Hefei, China). The Fe isotopic composition data were analyzed using the sample-standard bracketing approach to correct instrumental mass bias and time drifts. For this analysis, the samples were nebulized with a wet plasma, using a quartz dual cyclonic-spray chamber and a PFA MicroFlow Teflon nebulizer with an uptake rate of 50 μL min<sup>-1</sup>, and interferences (e.g., <sup>40</sup>Ar<sup>14</sup>N<sup>+</sup> and <sup>40</sup>Ar<sup>16</sup>O<sup>+</sup>) were resolved in the high-resolution mode. A detailed description of the Fe isotope measurement has been previously reported [28]. Each sample was analyzed three times. Additionally, the long-term external reproducibility of the instrument was 0.05‰ (2 SD) for <sup>δ</sup><sup>56</sup>Fe based on replicate runs of the in-house standards (UIFe and GSB). UIFe was a high-purity Fe solution obtained from the University of Illinois at Urbana-Champaign, and GSB was an ultrapure single elemental standard solution from the China Iron and Steel Research Institute. The long-term averages <sup>δ</sup><sup>56</sup>Fe of UIFe and GSB were 0.69 ± 0.05‰ (2 SD, n = 663) and 0.72 ± 0.05‰ (2 SD, n = 391). The values of the <sup>δ</sup><sup>56</sup>Fe based on U.S. Geological Survey (USGS) rock standards (BHVO-2, W-2, and AGV-2) were 0.12 ± 0.04‰ (2 SD, n = 3), 0.05 ± 0.02‰ (2 SD, n = 3), and 0.11 ± 0.05‰ (2 SD, n = 3). These results were identical within error to those reported in literature [29].

#### 2.4. Notation

The Fe isotopic compositions were reported using the standard delta notation expressed in per mil (‰) relative to the international Fe isotope standard (IRMM-014) according to Eq. 1.

$$\delta^{56}\text{Fe} = \left[ \frac{(^{56}\text{Fe}/^{54}\text{Fe})_{\text{sample}}}{(^{56}\text{Fe}/^{54}\text{Fe})_{\text{standard}}} - 1 \right] \times 1000 \quad (1)$$

The Fe isotope fractionation between two components, A and B (<sup>Δ</sup><sup>56</sup>Fe<sub>A-B</sub>), was expressed according to Eq. 2, and its precision was estimated by propagating the standard errors associated with the (<sup>δ</sup><sup>56</sup>Fe)<sub>A</sub> and (<sup>δ</sup><sup>56</sup>Fe)<sub>B</sub> values.

$$\Delta^{56}\text{Fe}_{A-B} = (\delta^{56}\text{Fe})_A - (\delta^{56}\text{Fe})_B \quad (2)$$

The Fe isotopic composition of the total plant was obtained using Eq. 3, where *i* represents different rice plant tissues, including the root, stems, leaves, panicles, husks, and seeds, *m* represents the dry mass of the tissues, and *c* represents the Fe concentration.

$$\delta^{56}\text{Fe}_{\text{plant}} = \frac{\sum_i m_i c_i \delta^{56}\text{Fe}_i}{\sum m_i c_i} \quad (3)$$

### 3. Results

#### 3.1. Fe isotope fractionation in soils

The Fe concentrations and Fe isotopic compositions of the three groups of individual plants (A, B, C) at the jointing and mature stages

were measured (Table S1). As shown in Fig. 1(a) and (b), the Fe concentrations of the soil at the jointing and mature stages were 22.2 g kg<sup>-1</sup> (2.2%) and 17.2 g kg<sup>-1</sup> (1.7%), respectively. At the jointing stage, the soil <sup>δ</sup><sup>56</sup>Fe value was 0.15 ± 0.03‰. The <sup>δ</sup><sup>56</sup>Fe value of the HCl-extracted soil extract was 0.20 ± 0.01‰, while that of the residual soil was 0.17 ± 0.05‰ (Table S1, Fig. 1(c) and 1(d)), indicating that the protocol for soil HCl-extraction did not bring about significant Fe isotope fractionation. The Fe in pore water primarily resulted from the dissolution of soil Fe, and the Fe isotope fractionation between pore water and soil (<sup>Δ</sup><sup>56</sup>Fe<sub>water-soil</sub>) was -0.29 ± 0.05‰, indicating that pore water was enriched in light Fe isotopes. Additionally, iron concentration of Fe plaque was determined according to the ratio of Fe content in Fe plaque extract to the dry mass of the roots [30]. Iron concentrations of Fe plaque were 92.3 g kg<sup>-1</sup> and 73.9 g kg<sup>-1</sup> at the jointing and mature stages, respectively, which were similar to iron concentrations of Fe plaque in Garnier et al. 2017 [13]. The <sup>δ</sup><sup>56</sup>Fe of the Fe plaque was 1.27 ± 0.08‰, and the Fe isotope fractionation between it and pore water (<sup>Δ</sup><sup>56</sup>Fe<sub>plaque-water</sub>) was 1.40 ± 0.08‰, indicating that the <sup>δ</sup><sup>56</sup>Fe became significantly heavier in the Fe plaque. At the maturity stage, the <sup>δ</sup><sup>56</sup>Fe values of the soil, the HCl-extracted Fe, the residual soil after extraction, and the Fe plaque were similar to those observed at the jointing stage. The plaque was not still attached to the roots after Fe plaque extraction in this study. The Fe plaque was pronouncedly enriched in heavier Fe isotopic composition relative to cortex. Therefore, if Fe plaque is still attached to the cortex, <sup>δ</sup><sup>56</sup>Fe of cortex will increase and the <sup>δ</sup><sup>56</sup>Fe of cortex and stele will be different.

#### 3.2. Fe isotope fractionation in roots and bulk rice plants

The results of the mass balance calculations revealed that the Fe concentrations of the bulk rice plants at the jointing and mature stages were 747 and 425 mg kg<sup>-1</sup>, respectively, and those of the roots at the jointing and mature stages were 13.3 and 13.7 g kg<sup>-1</sup>, respectively, which were the highest considering all the different rice plant tissues (Table S2, Fig. 2(a) and (b)). The Fe concentrations of the cortex were significantly higher than those of the stele. Furthermore, at the jointing and maturity stages, the <sup>δ</sup><sup>56</sup>Fe values of the rice plants were 0.46 ± 0.21 and 0.51 ± 0.14‰, respectively (Table S2, Fig. 2(c) and (d)), and for the roots, they were 0.67 ± 0.27 and 0.75 ± 0.03‰, respectively, which were the heaviest considering all the different rice plant tissues. At the jointing and maturity stages, the <sup>δ</sup><sup>56</sup>Fe values of stele were 0.89 ± 0.06 and 0.85 ± 0.34‰, respectively, while those of the cortex were 0.63 ± 0.24 and 0.75 ± 0.01‰, respectively, indicating that the <sup>δ</sup><sup>56</sup>Fe values of the cortex and the stele were identical within error.

#### 3.3. Fe isotope fractionation in above-ground rice plant parts (shoots)

The Fe concentrations of all the above-ground parts of the rice plants, including stems, leaves, panicles, husks, and seeds, at the jointing and mature stages are shown in Table S3, Fig. 3(a) and (c). The Fe concentrations in the various organs of the above-ground parts ranged between 16 and 610 mg kg<sup>-1</sup> at both the jointing and mature stages. The accumulation of Fe in the lower stem was higher than that in the upper stem; however, it was pronouncedly higher in old leaves than in new leaves at both the jointing and mature stages. Additionally, at the jointing and mature stages, all the rice plant tissues showed similar <sup>δ</sup><sup>56</sup>Fe values (Table S3, Fig. 3(c) and (d)), and at both the jointing and mature stage, the average <sup>δ</sup><sup>56</sup>Fe value of the stems was the lightest considering all the above-ground plant tissues, with, respectively, -0.63 ± 0.09‰ and -0.64 ± 0.12‰. The values of <sup>δ</sup><sup>56</sup>Fe at different heights of the stems were identical within error, and the Fe isotope fractionation between the roots and the stems (<sup>Δ</sup><sup>56</sup>Fe<sub>root-stem</sub>) was 1.39 ± 0.13‰, indicating that <sup>δ</sup><sup>56</sup>Fe became significantly lighter during the translocation of Fe from the roots to the stems. Additionally, the <sup>δ</sup><sup>56</sup>Fe value of the leaves was -0.06 ± 0.12‰ averagely, and the Fe isotope fractionation between

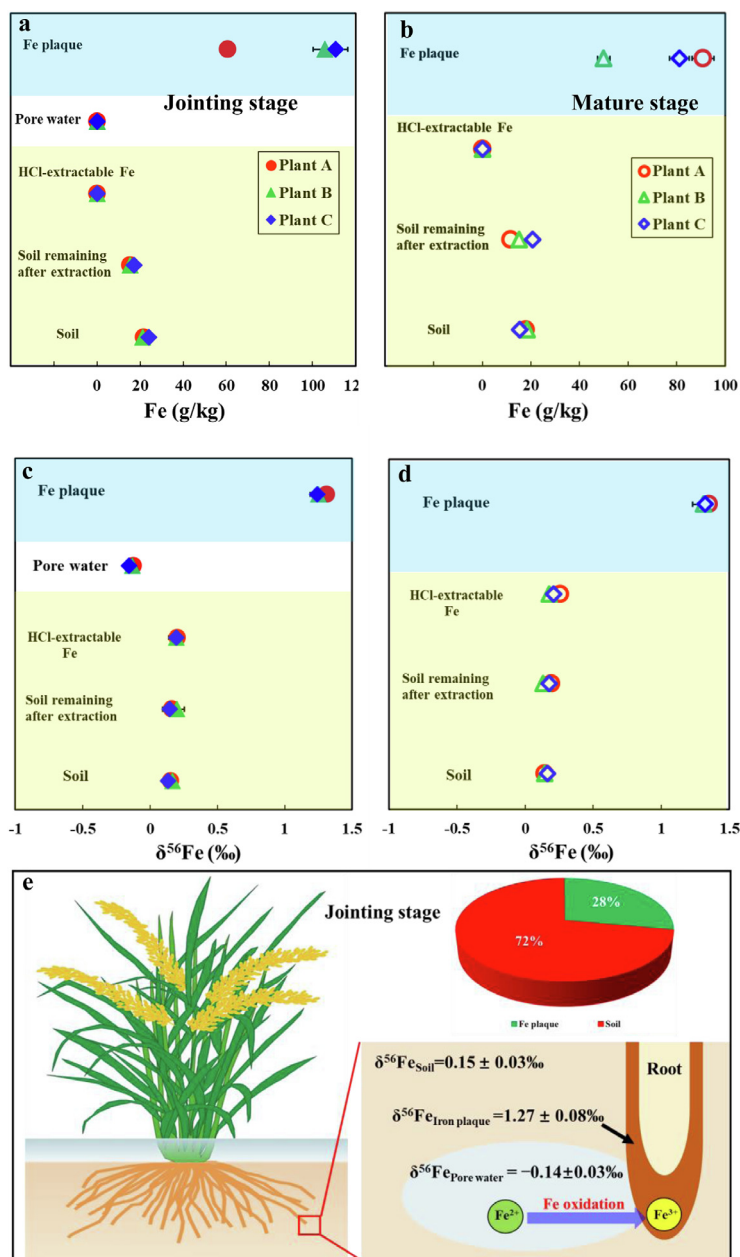


**Fig. 1.** (a) Fe concentrations in soil, pore water, and Fe plaque at the jointing stage; (b) Fe concentrations in soil and Fe plaque at the mature stage; (c) the  $\delta^{56}\text{Fe}$  values of soil, pore water, and Fe plaque at the jointing stage; (d)  $\delta^{56}\text{Fe}$  values of soil and Fe plaque at the mature stage; (e) mechanism of Fe fractionation during Fe(II) oxidation and formation of the Fe plaque. The pie chart represents the Fe sources in soil-rice systems based on Fe isotope fractionation and mass balance calculations.

the leaves and the stems ( $\Delta^{56}\text{Fe}_{\text{leaf-stem}}$ ) was  $0.52 \pm 0.18\text{‰}$ , indicating that the leaves were enriched in heavier Fe isotopes during Fe transport from the stems to the leaves. The  $\delta^{56}\text{Fe}$  value of the panicles was  $-0.23 \pm 0.01\text{‰}$ , and those of the grains, husks, and seeds at the mature stage were  $-0.17 \pm 0.18$ ,  $-0.25 \pm 0.36$ , and  $-0.09 \pm 0.04\text{‰}$ , respectively, indicating the  $\delta^{56}\text{Fe}$  values became heavier from husks to seeds. The  $\delta^{56}\text{Fe}$  values of the stems, leaves, and panicles at both the jointing and mature stages were similar, and the values of  $\Delta^{56}\text{Fe}_{\text{root-stem}}$  and  $\Delta^{56}\text{Fe}_{\text{leaf-stem}}$  were  $1.30 \pm 0.28\text{‰}$  and  $0.52 \pm 0.15\text{‰}$ , respectively.

## 4. Discussion

### 4.1. Iron migration and transformation in soil-water-plaque

**Soil→Water.** The Fe concentrations of the soil at the jointing and mature stages fell within the previously reported Fe concentration range

(~0.2–5%) for common soils [27]. At the jointing stage, the  $\delta^{56}\text{Fe}$  value of soil ( $0.15 \pm 0.03\text{‰}$ ) was similar to that reported by Liu et al. (2019) [11].

Iron-bearing minerals in soils can be transformed into bioavailable Fe via physiochemical and biological processes (e.g., proton-promoted dissolution, ligand-controlled dissolution, and reduction dissolution), and concomitantly the Fe isotope fractionation occurs accompanying the iron transformation processes. During proton-promoted dissolution, no obvious Fe isotope fractionation was observed. During ligand-promoted and reductive dissolution, Fe isotope fractionation was pronounced [31]. This is because during proton-promoted dissolution, the bonds between oxygen atoms and both detaching and adjacent Fe atoms were weakened, resulting in limited Fe isotope fractionation [31]. Additionally, equilibrium Fe isotope fractionation occurred during the ligand-controlled dissolution of the iron oxides and the dissolved Fe enriched

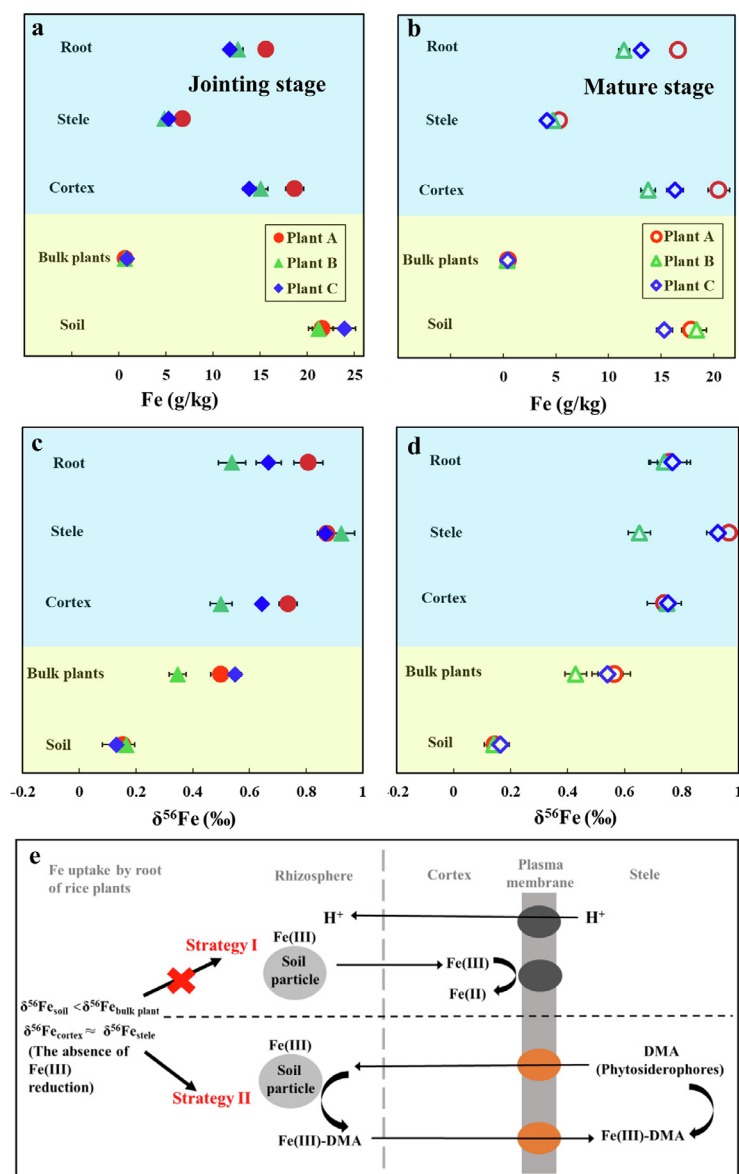


**Fig. 2.** Fe concentrations in roots (including cortexes and steles), bulk plants, and soil at (a) the jointing stage and (b) the mature stage. The  $\delta^{56}\text{Fe}$  values of roots (including cortexes and steles), bulk plants, and soil at (c) the jointing stage and (d) the mature stage. (e) Fe isotope fractionation between cortex and stele as well as that between the soil and bulk plants showing the rice plant Fe uptake mechanism.

in heavy Fe isotopes. The reductive dissolution of the iron oxides led to kinetic Fe isotope fractionation, resulting in the enrichment of the dissolved Fe with light Fe isotopes. The HCl-extracted iron, as a potential indicator of plant-available Fe in soil [27], includes the iron dissolved via the three processes described above. Reportedly, the  $\delta^{56}\text{Fe}$  values of HCl-extracted iron were  $\sim 0.2\text{--}0.3\text{‰}$  lighter than those of the bulk soil samples [13,27,32], and this may be attributed to the occurrence of reductive dissolution. However, in this study, HCl-extracted iron and the bulk soil samples showed similar  $\delta^{56}\text{Fe}$  values. The discrepancies among these authors suggest that such leaching experiments are insufficiently controlled (e.g., acid strength, temperature, time, and soil mineralogy) [33]. These results indicated that proton-promoted dissolution was dominant during soil dissolution in this study, and both ligand-controlled dissolution and reductive dissolution were negligible. Sorption can also cause significant Fe isotope fractionation between dissolved and sorbed Fe [34–36]. The similar Fe isotopic composition between the HCl-extracted soil extract and soil indicated that the effect of sorption on isotope fractionation during soil HCl-extraction

was not significant. The  $\delta^{56}\text{Fe}$  value of pore water was  $0.29\text{‰}$  lighter than that of the soil, indicating partial Fe(III) reduction may occur during Fe release from soil to pore water. The  $\delta^{56}\text{Fe}$  values of pore water may vary as a function of the relative proportions of dissolved Fe(II), adsorbed Fe(II), and the remaining Fe(III) during Fe(III) reduction [37].

**Water→Plaque.** The minerals in Fe plaque, which can be obtained from the root surface of the rice plants in the rhizosphere [30], are crystalline or amorphous Fe(III) (oxyhydr)oxides [38]. The precipitation of Fe(III) occurred mainly via abiotic and biotic Fe(II) oxidation in the surroundings of the roots; thus, the different Fe isotope fractionation processes in the plaque could be attributed to different Fe(II) oxidation processes (Fig. 1(e)). Regarding abiotic Fe(II) oxidation, the results of both laboratory and field studies suggested that the Fe isotope fractionation between aqueous Fe(II) and ferrihydrite was in the range  $\sim 0.9\text{--}1.0\text{‰}$  [39]; whereas for biotic Fe(II) oxidation using two cultures containing Fe(II)-oxidizing bacteria, the  $\delta^{56}\text{Fe}$  value of ferrihydrite was  $1.5\text{‰}$  heavier than that of the aqueous Fe(II) solution [40]. In this study, at the joint

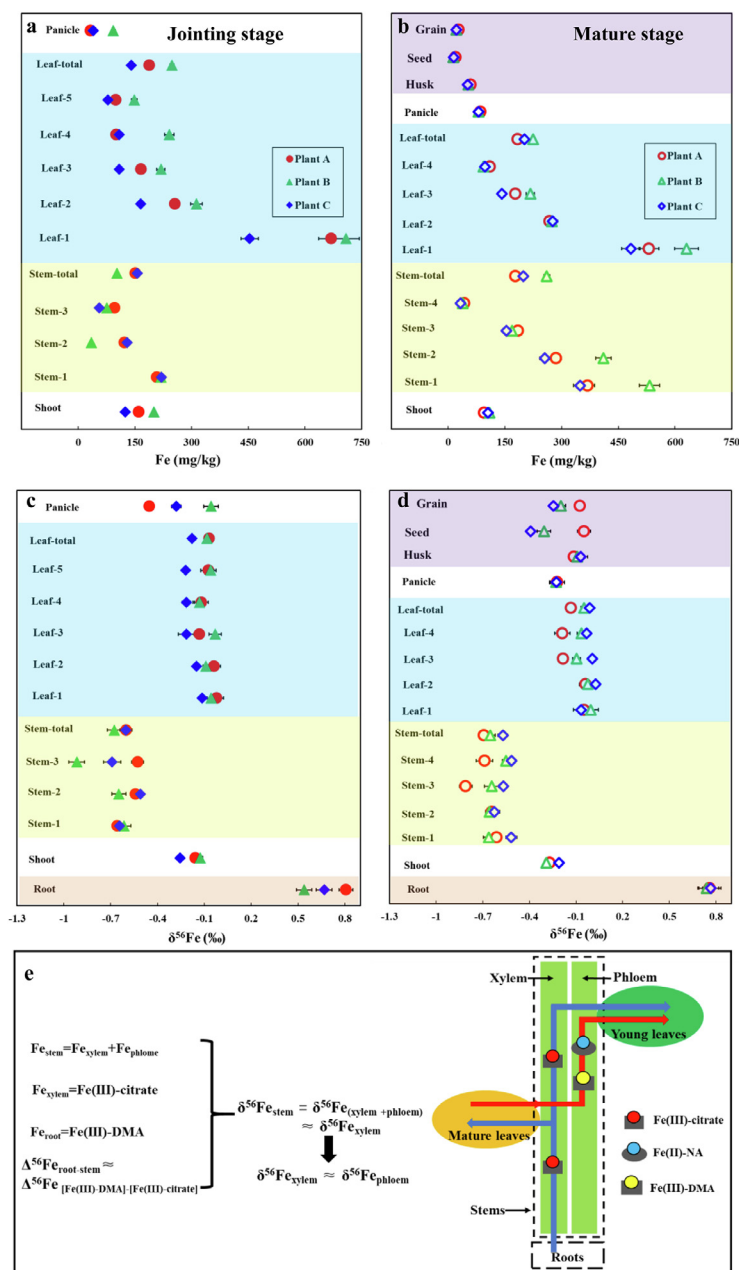


**Fig. 3.** Fe concentrations in different parts of the rice plants at (a) the jointing stage and (b) the mature stage. The  $\delta^{56}\text{Fe}$  values of different parts of the rice plants at (c) the jointing stage and (d) the mature stage. (e) Schematic illustration outlining Fe species and Fe translocation pathways through the xylem and phloem. In the xylem, Fe was translocated as Fe(III)-citrate, and in the phloem, Fe from mature leaves was re-mobilized as Fe(II)-NA and Fe(III)-DMA.

stage, the value of  $\Delta^{56}\text{Fe}_{\text{plaque-water}}$  ( $1.40 \pm 0.08\text{‰}$ ) was very close to the Fe isotope fractionation between Fe(II) and ferrihydrite for biotic Fe(II) oxidation but significantly higher than that for abiotic Fe(II) oxidation, indicating that the oxidation of Fe(II) in pore water to Fe(III) in plaque can be primarily attributed to the microbially-mediated Fe(II) oxidation processes. Sorption can also cause significant Fe isotope fractionation between dissolved and adsorbed Fe. In the presence or in the absence of silica and organic matter, heavy Fe preferentially sorbed to the ferrihydrite surface (e.g., goethite) and the remaining solution was enriched in lighter Fe isotopes [34–36]. Additionally, Fe(II) in the solution were also enriched in lighter Fe isotopes relative to adsorbed Fe(II) in the cell surface of bacteria [41]. Therefore, the Fe isotope fractionation between Fe plaque and pore water can be affected by sorption.

Ratio of Fe uptake from plaque and soil. Both Fe plaque and soil can serve as Fe sources for rice plants [42]; however, their relative con-

tributions are still unclear. Given that Fe plaque and soil have significantly different Fe isotopic compositions, their relative contributions as Fe sources can be quantified using a two endmember mixing model based on Eq. 4 and 5 [43],

$$X_{\text{soil}} + X_{\text{plaque}} = 100\% \quad (4)$$

$$X_{\text{soil}} \delta^{56}\text{Fe}_{\text{soil}} + X_{\text{plaque}} \delta^{56}\text{Fe}_{\text{plaque}} = \delta^{56}\text{Fe}_{\text{mix}} \quad (5)$$

, where  $X_{\text{soil}}$  and  $X_{\text{plaque}}$  represent the fraction of the soil pool and plaque pool, respectively, and  $\delta^{56}\text{Fe}_{\text{soil}}$ ,  $\delta^{56}\text{Fe}_{\text{plaque}}$ , and  $\delta^{56}\text{Fe}_{\text{mix}}$  represent the  $\delta^{56}\text{Fe}$  values of soil, Fe plaque, and a soil and plaque mixture, respectively. The Fe isotopic compositions of the whole plants were used to represent the isotope signature of the mixing reservoirs. The average  $\delta^{56}\text{Fe}$  values of the rice plants were  $0.46 \pm 0.21\text{‰}$  and  $0.51 \pm 0.14\text{‰}$  at the jointing and maturity stages, respectively. Based on the mixing

calculations performed using Eq. 4 and 5, the relative contributions of soil and the Fe plaque to rice plant Fe uptake in the field were 72% and 28% at the jointing stage, and 70% and 30% at the maturity stage, respectively (Fig. 1(e)). Therefore, the soil serves as the main source of the Fe taken up by rice plants. In Garnier et al. 2017 [13], Fe plaque was suggested as the main source of Fe uptake by the roots, considering the relatively high  $\delta^{56}\text{Fe}$  value of Fe plaque and low  $\delta^{56}\text{Fe}$  value of in the pore water.

#### 4.2. Iron uptake and translocation in roots

**Soil→Root.** The process of Fe translocation from the soil to the roots is a key step in the uptake of Fe by plants. For Strategy I-related plants, Fe(III) in the rhizosphere soils was reduced to Fe(II) before uptake into the root cells. For Strategy II-related plants, Fe(III) in rhizosphere soils was chelated by the plant-secreted ligand and dissolved before uptake. The Fe isotope fractionation between the soil and the bulk plants is an important signature that can be used to determine the Fe uptake strategy of plants [12,13,16]. Reportedly, for Strategy I-related plants, the bulk plants are slightly enriched in light Fe isotopes to a greater extent compared with the soil, and for Strategy II-related plants, the bulk plants are usually enriched in slightly heavy Fe isotopes relative to the bioavailable Fe in the soil. In this study, the  $\delta^{56}\text{Fe}$  values of the bulk rice plants were  $\sim 0.3\text{‰}$  heavier than those of the soil, indicating that Fe uptake from the soil to the roots probably occurred via Strategy II after the formation of the Fe(III)-DMA complex (Fig. 2(e)). DMA is a member of the mugenic acid family PS [23]. The molecular weight of Fe(III)-DMA complex is large [12]. Therefore, the relative mass differences of Fe-PS complex are small and the Fe-PS uptake should cause very minor Fe isotope fractionation [12]. This is consistent with the discussion about Fe isotope fractionation during Fe uptake. In the study of Arnold et al., 2015 [32], rice was grown in pots in a greenhouse under anaerobic and aerobic conditions. The rice plant shoots were slightly enriched in heavier Fe isotopes relative to the soil, indicating changes in the redox state of Fe occurring during Fe uptake in their experimental condition.

**Cortex→Stele.** During Fe uptake from the rhizosphere, Fe passes through the root cortex, and then reaches the stele (Fig. 2(e), Fig. S2). For Strategy I-related plants, Fe(III) reduction occurs during Fe uptake from the cortex to the stele owing to the action of plasma-membrane ferric reductases, while no Fe(III) reduction occurs during this process for Strategy II-related plants [8]. The results obtained in this study showed that Fe isotopic compositions between the stele and cortex were similar, indicating that during Fe translocation from the cortex to the stele under the conditions of this study, the reduction of Fe(III) was unlikely to occur (Fig. 2(e)). These findings are consistent with the conclusions regarding the Fe isotope fractionation between the rice plants and soil as discussed above. Once transported inside the cell, Fe(III) was still chelated by DMA. However, given that NA forms were also found to be complexed with Fe(III), it implies that Fe(III)-DMA was possibly transformed into Fe(III)-NA [8]. Reportedly, NA, with a structure similar to that of DMA, is the principal Fe chelator in root steles, and it plays an essential role in Fe transport in plants [44]. Both experimental investigations and *Ab initio* calculations have indicated a positive correlation between the Fe-ligand binding affinity and the equilibrium constant of the Fe isotope fractionation process [45, 46]. Heavier Fe isotopes are preferentially associated with stronger bonding environments [45], and the values of the stability constants (Log *K*) of Fe(III)-NA and Fe(III)-DMA are 20.6 and 18.1, respectively [47], implying a difference ( $\Delta\text{Log } K$ ) of 2.5. The corresponding  $\Delta^{56}\text{Fe}_{(\text{Fe(III)-NA}-(\text{Fe(III)-DMA})}$  value was  $\sim 0\text{‰}$  based on an experimental investigation of the linear trend between  $\Delta\text{Log } K$  and  $\Delta^{56}\text{Fe}$ , while the corresponding  $\Delta^{56}\text{Fe}_{(\text{Fe(III)-NA}-(\text{Fe(III)-DMA})}$  value was  $\sim 0.1\text{‰}$  based on the theoretically predicted linear trend between  $\Delta\text{Log } K$  and  $\Delta^{56}\text{Fe}$  [45]. These results indicate that the  $\delta^{56}\text{Fe}$  values of Fe(III)-NA and Fe(III)-DMA are similar. Thus, Fe could be chelated as

Fe(III)-DMA or Fe(III)-NA after its translocation from the cortex into the stele.

#### 4.3. Iron translocation in above-ground parts (shoots)

**Root→Stem.** After Fe uptake by the root system of the rice plants, the Fe is translocated to the stems via the xylem and phloem (Fig. 3(e), Fig. S2). Therefore, the contributions of both the xylem and phloem to Fe translocation should not be neglected [20]. Given that various Fe(III)-ligands (e.g., Fe(III)-citrate, Fe(III)-DMA, and Fe(III)-NA) are involved in the translocation process [23–25], Fe isotope fractionation would depend on the different types of Fe(III)-ligands involved. In xylem sap, Fe is translocated as Fe(III)-citrate [21]. However, the role of Fe(III)-ligand complexes in phloem sap is still unclear. Based on *Ab initio* calculations [15], the Fe isotope fractionation between the Fe(III)-citrate in the xylem and the Fe(III)-DMA in the roots was  $-1.43\text{‰}$ , which was similar to the  $\delta^{56}\text{Fe}$  value between the stems and the roots ( $\Delta^{56}\text{Fe}_{\text{stem-root}}$ ) observed in this study ( $-1.39 \pm 0.13\text{‰}$  and  $-1.30 \pm 0.28\text{‰}$  at the mature and jointing stages, respectively). The Fe isotopic composition of the stem was a mix of the Fe isotopic compositions of the phloem and the xylem. Thus, it can be considered that the xylem and the phloem have similar Fe isotopic compositions. Based on *Ab initio* calculations [15], Fe(II)-NA was pronouncedly enriched in light Fe isotopes by approximately  $-1.81\text{‰}$  relative to Fe(III)-citrate (xylem), while the Fe(III)-DMA was significantly enriched in heavy Fe isotopes by approximately  $+1.43\text{‰}$  relative to Fe(III)-citrate (xylem). Therefore, it is unlikely that a single form of Fe(III)-DMA or Fe(II)-NA was translocated from old leaves to new leaves or seeds via the phloem. Hence, it could be reasonably proposed that the Fe(III)-DMA and Fe(II)-NA mixture was transported in the phloem, resulting in an overall Fe isotopic composition that was similar to that of Fe(III)-citrate (Fig. 3(e)). Similar Fe isotopic compositions between the xylem and the phloem also indicated a quantitative transfer of mixture of Fe(III)-DMA and Fe(II)-NA in the phloem sap.

**Stem→Leaf→Seed.** During Fe translocation from stems to leaves, it was transformed into the Fe(III)-ferritin complex and stored in the leaf plastids. Ferritin, which consists of a hollow protein shell, stores 5,000 Fe atoms as Fe(III) [19]. In leaf tissues, Fe(III)-ferritin is a vital Fe source for the biosynthesis of Fe-containing proteins during photosynthesis, and it plays an important role in Fe translocation [22]. The Fe(III)-ferritin complex in leaves can be re-mobilized into the Fe(III)-DMA or Fe(II)-NA forms, then translocated from the lower leaves to upper leaves and seeds via the phloem sap, and ultimately transformed into the Fe(III)-ferritin complex, which is then stored in new leaves and seeds (Fig. S2) [8,19]. Hence, the different Fe isotopic compositions of the aboveground parts could be primarily attributed to the different types of Fe-ligands they contain. Since Fe is primarily stored in leaves as Fe(III)-ferritin, different leaves showed no significant difference in Fe isotopic compositions, and the  $\Delta^{56}\text{Fe}_{\text{stem-leaf}}$  value indicated that the Fe isotope fractionation between Fe(III)-ferritin and Fe(III)-citrate could be approximated as  $0.52\text{‰}$ .

## 5. Conclusions

The Fe uptake strategy (I and II), the Fe translocation in different tissues, and the transformation of various Fe ligands in xylem and phloem were clearly marked by using this Fe isotope tracer. Both  $\Delta^{56}\text{Fe}_{\text{soil-plant}}$  and  $\Delta^{56}\text{Fe}_{\text{cortex-stele}}$  values indicated that no Fe(III) reduction was observed before Fe uptake, which occurred via the Fe(III)-PS complex. The  $\Delta^{56}\text{Fe}_{\text{root-stem}}$  values at both the jointing and mature stages were similar to those between Fe(III)-citrate and Fe(III)-DMA obtained based on previous *Ab initio* calculations. These results indicate that Fe is transported as Fe(III)-DMA and Fe(II)-NA in the phloem and as Fe(III)-citrate in the xylem. The application of Fe isotope signatures can provide a better understanding of the mechanistic basis of Fe uptake and translocation in soil-rice plants systems, furthering our understanding of Fe biogeochemistry cycling in the environment.

## Declaration of Competing Interest

The authors declare that they have no conflict of interest.

## Acknowledgments

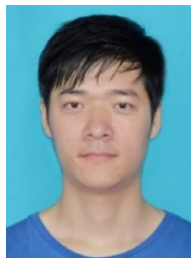
This work was supported by the National Natural Science Foundation of China (Grant Nos. 41807026, 42030702, and U20A20109), China Postdoctoral Science Foundation (Grant Nos. 2020T130126 and 2019M662820), Guangdong Key Research and Development Project (Grant Nos. 2019B110207002), Local Innovative and Research Teams Project of Guangdong Pearl River Talents Program (Grant Nos. 2017BT01Z176), projects of Science and Technology Development in Guangdong Academy of Sciences (Grant Nos. 2020GDASYL-20200104022 and 2019GDASYL-0103054), and Guangdong Special Support Plan for High-Level Talents (Grant Nos. 2017TX04Z175).

## Supplementary materials

Supplementary material associated with this article can be found, in the online version, at doi:10.1016/j.fmre.2021.04.006.

## References

- [1] S.A. Kim, M.L. Guerinot, Mining iron: iron uptake and transport in plants., *FEBS let* 581 (12) (2007) 2273–2280.
- [2] Y. Ishimaru, M. Suzuki, T. Tsukamoto, et al., Rice plants take up iron as an Fe<sup>3+</sup>-phytosiderophore and as Fe<sup>2+</sup>, *Plant J.* 45 (3) (2006) 335–346.
- [3] N.J. Robinson, C.M. Procter, E.L. Connolly, et al., A ferric-chelate reductase for iron uptake from soils, *Nature* 397 (1999) 694–697.
- [4] S.i. Takagi, K. Nomoto, T. Takemoto, Physiological aspect of mugineic acid, a possible phytosiderophore of graminaceous plants, *J. Plant Nutr.* 7 (1-5) (1984) 469–477.
- [5] R. Banakar, A.A. Fernandez, C. Zhu, et al., The ratio of phytosiderophores nicotianamine to deoxymugenic acid controls metal homeostasis in rice, *Planta* 250 (4) (2019) 1339–1354.
- [6] M.B. Zimmermann, R.F. Hurrell, Improving iron, zinc and vitamin A nutrition through plant biotechnology, *Curr. Opin. Biotechnol.* 13 (2) (2002) 142–145.
- [7] M. Yamauchi, Rice bronzing in Nigeria caused by nutrient imbalances and its control by potassium sulfate application, *Plant Soil* 117 (2) (1989) 275–286.
- [8] R. Hell, U.W. Stephan, Iron uptake, trafficking and homeostasis in plants, *Planta* 216 (4) (2003) 541–551.
- [9] W. Armstrong, Rhizosphere oxidation in rice: An analysis of intervarietal differences in oxygen flux from the roots, *Physiol. Plant.* 22 (2) (1969) 296–303.
- [10] K. Bashir, Y. Ishimaru, N.K. Nishizawa, Iron uptake and loading into rice grains, *Rice* 3 (2-3) (2010) 122–130.
- [11] C. Liu, T. Gao, Y. Liu, et al., Isotopic fingerprints indicate distinct strategies of Fe uptake in rice, *Chem. Geol.* 524 (2019) 323–328.
- [12] M. Guelke, F. Von Blanckenburg, Fractionation of stable iron isotopes in higher plants, *Environ. Sci. Technol.* 41 (6) (2007) 1896–1901.
- [13] J. Garnier, J. Garnier, C. Vieira, et al., Iron isotope fingerprints of redox and biogeochemical cycling in the soil-water-rice plant system of a paddy field, *Sci. Total Environ.* 574 (2017) 1622–1632.
- [14] N. Dauphas, S.G. John, O. Rouxel, Iron isotope systematics, *Rev. Mineral. Geochem* 82 (1) (2017) 415–510.
- [15] F. Moynier, T. Fujii, K. Wang, et al., Ab initio calculations of the Fe (II) and Fe (III) isotopic effects in citrates, nicotianamine, and phytosiderophore, and new Fe isotopic measurements in higher plants, *CR Geosci.* 345 (5) (2013) 230–240.
- [16] M. Kiczka, J.G. Wiederhold, S.M. Kraemer, et al., Iron isotope fractionation during Fe uptake and translocation in alpine plants, *Environ. Sci. Technol.* 44 (16) (2010) 6144–6150.
- [17] F. von Blanckenburg, N. von Wirén, M. Guelke, et al., Fractionation of metal stable isotopes by higher plants, *Elements* 5 (6) (2009) 375–380.
- [18] M. Guelke-Stelling, F. von Blanckenburg, Fe isotope fractionation caused by translocation of iron during growth of bean and oat as models of strategy I and II plants, *Plant soil* 352 (1-2) (2012) 217–231.
- [19] H. Marschner, *Mineral Nutrition of Higher Plants*, Second Edition, Academic Press, London, 1995.
- [20] T. Yoneyama, T. Goshio, M. Kato, et al., Xylem and phloem transport of Cd, Zn and Fe into the grains of rice plants (*Oryza sativa* L.) grown in continuously flooded Cd-contaminated soil, *Soil Sci. Plant Nutr.* 56 (3) (2010) 445–453.
- [21] A. Pich, G. Scholz, U.W. Stephan, Iron-dependent changes of heavy metals, Nicotianamine, and citrate in different plant organs and in the xylem exudate of two tomato genotypes. Nicotianamine as possible copper translocator, *Plant Soil* 165 (2) (1994) 189–196.
- [22] J.-F. Briat, C. Curie, F. Gaymard, Iron utilization and metabolism in plants, *Curr. Opin. Plant Biol.* 10 (3) (2007) 276–282.
- [23] S. Mori, Iron acquisition by plants, *Curr. Opin. Plant Biol.* 3 (2) (1999) 250–253.
- [24] R. Nishiyama, M. Kato, S. Nagata, et al., Identification of Zn–nicotianamine and Fe–2'-deoxymugineic acid in the phloem sap from rice plants (*Oryza sativa* L.), *Plant Cell Physiol* 53 (2) (2012) 381–390.
- [25] S. Koike, H. Inoue, D. Mizuno, et al., OsYSL2 is a rice metal-nicotianamine transporter that is regulated by iron and expressed in the phloem, *Plant J* 39 (3) (2004) 415–424.
- [26] M. Kato, S. Ishikawa, K. Inagaki, et al., Possible chemical forms of cadmium and varietal differences in cadmium concentrations in the phloem sap of rice plants (*Oryza sativa* L.), *Soil Sci. Plant Nutr.* 56 (6) (2010) 839–847.
- [27] M. Guelke, F. von Blanckenburg, R. Schoenberg, et al., Determining the stable Fe isotope signature of plant-available iron in soils, *Chem. Geol.* 277 (3–4) (2010) 269–280.
- [28] X. Ding, E.M. Ripley, W. Wang, et al., Iron isotope fractionation during sulfide liquid segregation and crystallization at the Lengshuiqing Ni-Cu magmatic sulfide deposit, SW China, *Geochim. Cosmochim. Acta* 261 (2019) 327–341.
- [29] P.R. Craddock, N. Dauphas, Iron isotopic compositions of geological reference materials and chondrites, *Geostandards Geoanal. Res.* 35 (1) (2011) 101–123.
- [30] F.Y. Jiang, X. Chen, A.C. Luo, Iron plaque formation on wetland plants and its influence on phosphorus, calcium and metal uptake, *Aquat. Ecol.* 43 (4) (2009) 879–890.
- [31] J.G. Wiederhold, S.M. Kraemer, N. Teutsch, et al., Iron isotope fractionation during proton-promoted, ligand-controlled, and reductive dissolution of goethite, *Environ. Sci. Technol.* 40 (12) (2006) 3787–3793.
- [32] T. Arnold, T. Markovic, G.J. Kirk, et al., Iron and zinc isotope fractionation during uptake and translocation in rice (*Oryza sativa*) grown in oxic and anoxic soils, *CR Geosci* 347 (2015) 397–404.
- [33] B. Wu, W. Amelung, Y. Xing, et al., Iron cycling and isotope fractionation in terrestrial ecosystems, *Earth Sci. Rev.* (2018).
- [34] P. Chanda, Z. Zhou, D.E. Latta, et al., Effect of organic C on stable Fe isotope fractionation and isotope exchange kinetics between aqueous Fe (II) and ferrihydrite at neutral pH, *Chem. Geol.* 531 (2020) 119344.
- [35] G. Icopini, A. Anbar, S. Ruebush, et al., Iron isotope fractionation during microbial reduction of iron: the importance of adsorption, *Geology* 32 (3) (2004) 205–208.
- [36] L. Wu, E.M. Percak-Dennett, B.L. Beard, et al., Stable iron isotope fractionation between aqueous Fe (II) and model Archean ocean Fe–Si coprecipitates and implications for iron isotope variations in the ancient rock record, *Geochim. Cosmochim. Acta* 84 (2012) 14–28.
- [37] H.A. Crosby, E.E. Roden, C.M. Johnson, et al., The mechanisms of iron isotope fractionation produced during dissimilatory Fe (III) reduction by *Shewanella putrefaciens* and *Geobacter sulfurreducens*, *Geobiology* 5 (2007) 169–189.
- [38] C.M. Hansel, S. Fendorf, S. Sutton, et al., Characterization of Fe plaque and associated metals on the roots of mine-waste impacted aquatic plants, *Environ. Sci. Technol.* 35 (19) (2001) 3863–3868.
- [39] T.D. Bullen, A.F. White, C.W. Childs, et al., Demonstration of significant abiotic iron isotope fractionation in nature, *Geology* 29 (8) (2001) 699–702.
- [40] L.R. Crael, C.M. Johnson, B.L. Beard, et al., Iron isotope fractionation by Fe (II)-oxidizing photoautotrophic bacteria, *Geochim. Cosmochim. Acta* 68 (6) (2004) 1227–1242.
- [41] D.S. Mulholland, F. Poitrasson, L.S. Shirokova, et al., Iron isotope fractionation during Fe(II) and Fe(III) adsorption on cyanobacteria, *Chem. Geol.* 400 (2015) 24–33.
- [42] A. Sebastian, M. Prasad, Iron plaque decreases cadmium accumulation in *Oryza sativa* L. and serves as a source of iron, *Plant Biol* 18 (6) (2016) 1008–1015.
- [43] J.G. Wiederhold, Metal stable isotope signatures as tracers in environmental geochemistry, *Environ. Sci. Technol.* 49 (5) (2015) 2606–2624.
- [44] I. Beneš, K. Schreiber, H. Ripberger, et al., Metal complex formation by nicotianamine, a possible phytosiderophore, *Experientia* 39 (3) (1983) 261–262.
- [45] J.L. Morgan, L.E. Wasylenki, J. Nuester, et al., Fe isotope fractionation during equilibration of Fe–organic complexes, *Environ. Sci. Technol.* 44 (16) (2010) 6095–6101.
- [46] G. Ottonello, M. Vetuschi Zuccolini, The iron-isotope fractionation dictated by the carboxylic functional: an ab-initio investigation, *Geochim. Cosmochim. Acta* 72 (24) (2008) 5920–5934.
- [47] N. von Wirén, S. Klair, S. Bansal, et al., Nicotianamine chelates both Fe(III) and Fe(II): implications for metal transport in plants, *Plant Physiol* 119 (3) (1999) 1107–1114.



Guojun Chen obtained his Ph.D. degree from the University of Science and Technology of China in 2018, and received postdoctoral training at the Institute of Eco-environmental Science and Soil Sciences, Guangdong Academy of Sciences during 2018–2020. His research interests focus on utilizing Fe-N-O isotopic analysis to understand Fe-N biogeochemical cycles and Cr isotopic analysis to understand microbial Cr(VI) reduction.



Fangbai Li is a professor of environmental soil chemistry and general director at the Institute of Eco-environmental and Soil Sciences, Guangdong Academy of Sciences. His major research interests are Fe, C, N, As, and Cd redox cycling and the mechanism of microbe-mineral interactions.